19EC Debris Coolability and Core Concrete Interaction

Appendix 19E of the ABWR PRA discusses core concrete interaction. In particular, in Subsection 19E.2.1.3.6, it is stated that the core debris will be quenched preventing substantial concrete ablation due to operation of the passive flooder. Even if the flooder was assumed to fail, water from the suppression pool would flood the lower drywell after 20.32 cm (8 inches) of radial ablation had occurred. This conclusion was based on available experimental information and the work performed in IDCOR Subtask 15.2 (Reference 19EC-1).

Since the original ABWR PRA was submitted there has been continued research in the areas of debris coolability and core concrete interaction. Experiments performed at Argonne as part of the MACE program have indicated that, due to crust formation, debris cooling may be limited. This section will investigate the uncertainties associated with debris coolability in the lower drywell of the ABWR. The investigation will begin with a look at applicable experimental data. Next, the issue of debris coolability will be decomposed into the controlling parameters and followed by the development of a decomposition event tree (DET). After creation of the DET, deterministic evaluations will be made to quantify the end points of the tree. Finally, sensitivities to key assumptions will be investigated.

19EC.1 Applicability of Experiments to ABWR

Several experiments have been carried out to investigate the influence of an overlying water pool on debris coolability. The critical parameter that appears to dominate the behavior in several of the experiments is the formation of a stable crust. This crust is found to prevent substantial water ingression and, therefore, debris cooling. The major criticism of these experiments is that, due to their small scale, a stable crust is preferentially formed. This limitation makes it quite difficult to extrapolate the results to a large reactor cavity. The MACE tests at Argonne have attempted to address this weakness by investigating larger cavity designs.

The following provides a brief summary of several debris coolability experiments.

(1) Theofanous and Saito - 1980 (Reference 19EC-2)

Experiments were performed with liquid nitrogen and water and liquid nitrogen and Freon 11. Crust formation was observed at low gas velocities but found to become unstable at high sparging rates. It was observed that as the gas velocity increased to a magnitude typical of core-concrete interaction, the heat transfer rate increased by a factor of ten. The heat transfer rates were found to approach those associated with critical heat flux.

(2) Greene - 1988 (Reference 19EC-3)

Tests were run with liquid metals with water and Freon R11. Gases were injected in the melt. It was observed that the water/melt interactions were generally unstable and

that the upward heat transfer increased with gas velocity. The typical upward heat transfer rates were found to be 6 times greater than the classical Berenson correlation.

(3) FRAG (Reference 19EC-4)

This series of tests performed at Sandia National Laboratories (SNL) used 3 mm diameter steel spheres heated and placed in a 20 cm diameter concrete crucible. Tests were performed both with and without water addition. Both limestone and basaltic concrete types were investigated. The limestone tests showed that a stable crust made of concrete and steel formed that kept the water from penetrating the rest of the debris bed. The basaltic concrete allowed for some water penetration. The conclusion from these tests was that core-concrete attack continued even in the presence of water and that a substantial amount of steel oxidation took place.

(4) SWISS (Reference 19EC-5)

These tests, also performed at SNL, involved the interaction of molten steel on limestone concrete. The steel was heated at approximately five times the expected reactor decay heat levels. There appeared to be no violent melt-water interactions and the melt did not quench. There was a stable crust that was found to attach to the MgO sidewall. Typical upward heat flux was 800 kW/m^2. There was also information from the experiment that the overlying water pool provided substantial aerosol scrubbing (DFs of 10-30).

(5) Mark I Shell Failure Experiments (Reference 19EC-6)

Several experiments were carried out Fauske and Associates, Inc. to investigate the influence of water on debris coolability and specifically to observe drywell shell heatup. Iron-alumina thermite was discharged onto a concrete slab pre-flooded with water. The initial heat transfer was found to be quite high (20 times CHF) and leveled off at about 800 kW/m^2 later.

(6) MACE (Reference 19EC-7)

A series of large-scale experiments are being performed at Argonne National Laboratory investigating the coolability of molten-corium by water during its interaction with concrete. The MACE program has attempted to

(a) Employ prototypic corium melt materials

(b) Employ prototypic concrete types

(c) Obtain realistic melt temperatures

(d) Obtain realistic MCCI initial conditions

(e) Include prototypic chemical and internal heating, and by the increased size

(f) Ensure applicability to reactor cavities

In the scoping test, a high initial heat removal was observed. The crust that was formed was found to be supported by the electrodes. There were periodic melt eruptions through the crust that lead to substantial melt quenching. However, the melt did not completely cool and continued to erode concrete. One of the major difficulties with the test was that there were larger than prototypic heating rates.

The next test, M1, was performed on November 25, 1991. The major difficulty with this test was that not all of the material melted initially and the sintered region on the top kept the water from penetrating the melt. Low melt-water heat transfer rates were observed. Concrete attack continued with the debris not cooled. This sintered crust configuration is not prototypical of the ABWR.

The most recent test, M1B, corrected the problems encountered with M1. The melt temperature was observed to decrease steadily to near the concrete liquidus temperature after the water was introduced. Concrete ablation was found to continue but at a reduced rate (a few mm/h). The post-test examination showed that there were large holes in the top surface.

The experiments described above are insufficient to enable a full understanding of debris coolability in the lower drywell of the ABWR. Some insights can, however, be extracted. The following shows the observed upward heat flux for three of the tests.

SWISS	- 800 kW/m^2
Mark I Shell Test	- 800 kW/m^2
MACE Scoping	- 600 kW/m^2

One of the major reasons why these tests are not prototypic is that, due to their small scale, they promote a stable crust formation. The larger scale MACE tests should generate some useful insights.

19EC.2 Description of Event Tree Analysis

19EC.2.1 Debris Coolability

A decomposition event tree (DET), shown in Figure 19EC-1, was developed to assess the likelihood of debris coolability. This subsection describes the branch points and the quantification of this DET.

19EC.2.1.1 Fraction of Debris in Lower Drywell Early (COR_DW_E)

This event assesses the initial debris mass which relocates to the lower drywell soon after vessel failure. The amount of debris which enters the lower drywell early is dependent on the amount of debris molten in the lower RPV head at the time of RPV failure and on the amount of

entrainment of the debris from the lower drywell. However, for simplicity, debris entrainment to the upper drywell was conservatively neglected in this analysis. For consistency with the DCH analysis, two regimes are considered for the fraction of the core inventory which is molten in the RPV at the time of RPV failure (Subsection 19EA.2.1.4). These regimes are:

Low 0 - 20% (nominal 10%) melt fraction - 0.9 probability

High 20 - 60% (nominal 40%) melt fraction - 0.1 probability

19EC.2.1.2 Amount of Initial Debris Superheat (SUP_HEAT)

This event is used to represent the initial debris temperature when the debris first contacts the lower drywell floor. It is also used as a surrogate to represent the additional metal/water reaction heat production associated with a high metal to oxide ratio in the debris. Superheated debris or debris with a high metal content is expected to be more difficult to quench initially and to experience faster initial concrete erosion. In the deterministic CCI analysis discussed in Subsection 19EC.3, the low superheat cases are represented by (molten) debris at the U-Zr-O eutectic melting temperature (approximately 2500 K). High superheat was taken to be temperatures in the range 300-500 K above the melting temperature. This was represented in the deterministic analysis by increasing the amount of steel added to the melt prior to vessel breach.

Two cases were considered in the DET analysis. The first case represents sequences with a small amount (10% of core inventory) of molten debris in the lower plenum at vessel rupture and the second case represents large amounts of debris (40%).

- Case 1—Small Debris Mass in Lower Drywell Early

For the case of a small debris mass in the lower RPV, it is likely that either

(1) Vessel failure occurred fairly quickly after core slump into the lower plenum, or that

(2) The debris in the lower plenum was initially quenched by residual water in the lower plenum and that RPV failure occurred later, after the water was boiled away and the debris started to reheat (BWRSAR-type failure model).

For these situations it is judged likely that the debris temperature will be at, or near, its melting point.

For the case of a large amount of molten debris it could be expected that this resulted from a delayed failure of the RPV allowing more debris to flow into the lower plenum or for melting and heating of quenched debris already relocated to the lower plenum (BWRSAR model). For both situations the extended time to vessel failure could result in higher molten debris temperatures at RPV failure. It is unclear what the actual debris temperature would be for this case. Hence, equal probabilities are assigned to each branch to represent this large uncertainty.

19EC.2.1.3 Debris Quenched Early (QUENCH_E)

The probability that long term debris cooling will be established is greatly increased if the initial debris pour is quenched soon after being expelled from the vessel. Initial quenching of the debris implies either that the debris has been fragmented to sizes which allow cooling, or if the debris is a continuous "pool" that it is sufficiently shallow to allow cooling by conduction through the layer of solid debris.

The ABWR design makes it extremely unlikely that water will be in the lower drywell prior to RPV failure. Most of the core damage frequency is initiated by a transient. This type of sequence would not result in water in the lower drywell at the time of vessel failure. Only a LOCA in the RPV bottom drain line or an accident in which a large mass of water is added to the containment before core damage would result in water entering the drywell. All other LOCAs blow down into the upper drywell (which drains directly to the suppression pool). Hence, water which enters the lower drywell coincident with the expelled debris must come from residual RPV inventory or from in-vessel injection systems which are operating at (or are initiated at) RPV failure. For a melt progression the lower plenum is nearly full of water at the time of vessel failure. Thus, 70,000 kg of water is available to quench the debris.

In addition, water may enter the lower drywell at the time of vessel failure via the passive flooder. If water from the vessel does not enter the cavity, the debris will rapidly heat the lower drywell, and the flooder will open quickly. For a BWRSAR type melt progression model, there will not be water in the lower plenum at the time of vessel failure. In this case, the lower drywell will heat up quickly and the passive flooder will open. A calculation was performed with a modified version of MAAP-ABWR, which simulates the BWRSAR melt progression model, described in Subsection 19EC.6. Case LATE indicates that the flooder will open about 30 minutes after vessel failure for this case. Thus, it is very likely that water will be available to quench the initial debris expelled from the vessel.

The major parameters judged to impact the probability of initial debris quenching are

(1) The mass of debris in the lower drywell following RPV failure

(2) The availability of water in the lower drywell

(3) The initial temperature of the debris

The mass of debris retained in the lower drywell is determined in a preceding event. The initial debris temperature is also determined in a prior event. The source of water depends on the presumed core melt progression model as described above. In a MAAP-type melt progression, the initial availability of water is assured. For a BWRSAR model, the water comes either from injection systems which begin to inject at vessel failure or from the operation of the flooder which is considered in the next node. Since no credit will be taken for early quenching if a significant amount of debris enters the cavity before lower drywell flooding occurs, the order

of this question and the late cavity flooding question (CAVWAT_L) question is not important for the BWRSAR case.

Four cases were defined in the DET. These cases are:

- Case 1—Small Debris Mass and Low Superheat

  For this case, approximately 24000 kg of molten debris are released from the RPV at vessel failure. Since the debris has a low superheat and the debris depth is very shallow (< 5 cm) it is highly likely that the debris would be initially quenched.

- Case 2—Small Debris Mass and High Superheat

  As for Case 1, approximately 24000 kg of molten debris are released from the RPV at vessel failure. In this case, the debris has a high superheat and, although the debris depth is very shallow (< 5 cm), it is somewhat less likely that the debris would be initially quenched when the lower drywell is flooded for this case than for Case 1.

- Case 3—Large Debris Mass and Low Superheat

  For this case, approximately 94000 kg of molten debris are released from the RPV at vessel failure. The debris depth in this case would be relatively shallow (< 15 cm). Since the debris pool is relatively shallow and the debris superheat is low, it is judged that it is likely to be initially quenched when the lower drywell is flooded.

- Case 4—Large Debris Mass and Low Superheat

  As for Case 3, approximately 94000 kg of molten debris are released from the RPV at vessel failure and the debris depth would be relatively shallow (< 15 cm). However, the debris superheat is high and it is judged to be indeterminate whether or not the debris will be quenched by residual RPV coolant inventory.

19EC.2.1.4 Water Enters Cavity Late (CAVWAT_L)

This parameter is used to represent the longer term addition of water to the lower drywell. The lower drywell water addition systems which are considered are the direct drive diesel firewater system, any vessel injection which is available late in the accident and the passive flooder. Initiation of the firewater addition system is the most likely means of late water addition to the lower drywell. If the firewater system is not started, the passive flooder system will begin to inject water when the fusible material, located at the ends of the pipes near the drywell floor, melts. The fusible material on the passive flooder system is assumed to open when the lower drywell gas temperature reaches 533 K (500°F). Assuming a BWRSAR melt progression model, the fusible valves on the passive flooder system would open in approximately 30 minutes. For a MAAP-type melt progression model, the water in the lower drywell is first boiled off. The debris then begins to heat up. If the debris is quenched during the early boil-off

phase the debris must reheat resulting in approximately 2 hours to flooder actuation. If the debris was not quenched early, the flooder opens about 30 minutes after the debris bed dries out. This event is a sorting type event, quantified (either 0 or 1) based on prior branch decisions in the CET.

19EC.2.1.5 Time Remaining Core Debris Falls Into Cavity (COREDROP)

This event assesses the timing of the entry of the remaining debris into the lower drywell relative to the timing of the addition of water (i.e., from the passive flooder or firewater system). If the majority of the debris is held up in the vessel until after water addition begins, then debris cooling is substantially more likely than if the bulk of the RPV debris enters the lower drywell prior to water addition. MAAP calculations indicate that the residual RPV debris will melt and fall into the lower drywell very slowly after vessel failure. This behavior is also typical of BWRSAR-type calculations (Reference 19EC-8).

Two cases are considered in the quantification of the event. The timing of residual RPV debris entry into the lower drywell is considered to be sensitive to the extent of the accident progression in-vessel at the time of vessel failure. For the case of a small amount of molten debris in the lower RPV plenum at RPV failure (Event 1 in this DET), it is inferred that RPV failure has occurred relatively “early” in the in-vessel accident progression process. Conversely, for a large amount of molten debris in the lower RPV plenum at RPV failure, it is more likely that the in-vessel accident progression is further advanced at the time of RPV failure. Consequently, it would be expected that for the case of small initial debris pours the timing between vessel failure and later debris pours would be delayed relative to the case of large initial debris pours. Based on insights from ABWR specific MAAP analyses and from a review of BWRSAR calculations for other BWR sequences branch probabilities were estimated.

19EC.2.1.6 Heat Transfer Rate to Overlying Water (HT_UPWARD)

This event assesses the longer term steady state heat transfer rate which characterizes upwards heat transfer from the debris. Three regimes are considered

(1) Heat transfer limited by hydrodynamics in an overlying water pool (CHF limit)

(2) Heat transfer limited by film boiling to an overlying water pool

(3) Heat transfer limited by conduction through a debris crust on the upper debris surface

Nominal values of the heat transfer rate used in the deterministic CCI model to characterize these three heat transfer regimes are 900, 300 and 100 kW/m^2, respectively.

The conduction limit represents conditions where a crust forms on the surface of the debris and water cannot penetrate into the debris bed. The use of a 100 kW/m^2 heat flux is believed to be very conservative. If the debris is not quenched and core concrete interaction occurs, the upper

crust will thin to a condition where the upward and downward heat fluxes are nearly equal. This will lead to a heat flux much higher than 100 kW/m^2. Therefore, this value will lead to very aggressive core concrete interaction. Further discussion of the upward heat flux for the conduction limited configuration is given in Subsection 19EC.3.1.

The hydrodynamic limit represents cases where water can penetrate into the debris bed allowing a much greater effective debris/coolant heat transfer area. Under these conditions the heat transfer rate is limited by the ability of the water to penetrate the debris bed. The use of 900 kW/m^2 is much lower than the typical heat fluxes observed in the experiments performed to date.

The film boiling regime is selected to represent an intermediate heat transfer rate where, for example, the crust is unstable allowing water to penetrate the debris bed in a limited fashion. The early phase of the experiments indicate a heat flux well in excess of 300 kW/m^2 before the formation of a crust.

Four cases were identified for quantification. These cases are described below.

- Case 1—Large Debris Mass in Lower Drywell Early, Debris Initially Quenched and Residual Core Debris Enters Lower Drywell After Flooding

  This case is considered the most favorable set of conditions for establishment of a particulated debris bed which would be conducive to water ingression and coolability. The initial phase of the interaction is characterized by a large amount of debris which is initially quenched in the lower drywell. Prior to the entry of the residual RPV debris, the lower drywell is flooded resulting in the residual debris pouring into a pool of water which is likely to lead to fragmentation, quenching and the establishment of a particle bed. Consequently, a high probability is assigned under these conditions to an upwards heat flux characteristic of a particle bed with water ingression.

- Case 2—Small Debris Mass in Lower Drywell Early, Debris Initially Quenched and Residual Core Debris Enters Lower Drywell After Flooding

  This case is considered to represent nearly as favorable a set of conditions for establishment of a particulated debris bed as was Case 1. In contrast to Case 1 however, the initial phase of the interaction is characterized by only a small amount of debris which is quenched in the lower drywell. Hence, a larger amount of debris enters the lower drywell after RPV failure than for Case 1. Prior to the entry of the residual RPV debris, the lower drywell is flooded resulting in the residual debris pouring into a pool of water which is likely to lead to fragmentation, quenching and the establishment of a particle bed. Consequently, as for Case 1, a relatively high probability is assigned under these conditions to an upwards heat flux characteristic of a particle bed with water ingression.

- Case 3—No Initial Debris Quench and Residual Core Debris Enters Lower Drywell After Flooding

  This case is considered less favorable for establishment of a particulated debris bed which would be conducive to water ingression and coolability. The initial phase of the interaction is characterized by failure to quench the debris soon after RPV failure. However, prior to the entry of the residual RPV debris, the lower drywell is flooded resulting in the residual debris pouring into a pool of water which is likely to lead to fragmentation of this debris. However, since the initial debris pour was not quenched, long term establishment of a coolable particulated debris bed is somewhat uncertain. Consequently, a lower probability has been assigned for the most favorable debris bed configuration compared with Cases 1 and 2.

- Case 4—Residual Core Debris Enters Lower Drywell Prior to Flooding

  This is considered the least favorable set of conditions for establishment of a particulated debris bed which would be conducive to water ingression and coolability. For this case the bulk of the residual core debris enters the lower drywell prior to lower drywell flooding. This could lead to formation of a molten pool undergoing concrete attack. Later water addition, instead of particulating the debris may lead to crust formation, limiting the ability of water to penetrate into the debris.

19EC.2.1.7 Core Debris Concrete Attack (CCI)

This event characterizes the nature of the debris concrete attack. Three branches are considered. The No CCI branch represents cases where the little or no debris concrete attack would be expected. Wet CCI represents cases where CCI occurs in the presence of an overlying water pool and Dry CCI is for cases where the lower drywell was not flooded.

- Case 1—Lower Drywell Not Flooded

  The Dry CCI case occurs for all sequences where both active injection and the passive flooder fail to supply water to the lower drywell after vessel failure. Under these conditions Dry CCI is assured.

- Case 2—Lower Drywell Flooded, Upward Heat Transfer Limited by CHF

  For cases where the lower drywell is flooded, MAAP analysis and supplemental hand calculations indicate that if the upward heat transfer is above about 300-400 kW/m^2 then the debris bed will be coolable.

- Case 3—Lower Drywell Flooded, Upward Heat Transfer Limited by Film Boiling

  For cases where the lower drywell is flooded, MAAP analysis and supplemental hand calculations indicate that if the upward heat transfer is in the range of about 300 kW/m^2 then the debris bed should be coolable. Since this case represents a range of upward heat transfer

regimes (200-400 kW/m^2) and the lower part of this range may not in all cases be coolable and probabilities were assigned accordingly.

- Case 4—Lower Drywell Flooded, Upward Heat Transfer Limited by Conduction

  For cases where the lower drywell is flooded, MAAP analysis and supplemental hand calculations indicate that if the upward heat transfer is below about 200 kW/m^2 then the debris bed will not be coolable.

19EC.2.2 Pedestal Resistance to CCI

This subsection describes the decomposition event tree (DET) analysis used to assess the probability of pedestal failure as a result of radial core concrete (CCI) attack in the lower drywell after reactor vessel failure. The DET is shown in Figure 19EC-2. Pedestal wall failure is considered to be sensitive to

(1) The nature of the CCI (i.e. whether wet or dry)

(2) Whether the debris spreads from lower drywell into the suppression pool following radial penetration through the pedestal wall to the wetwell/drywell connecting vents

(3) The extent of radial erosion compared to downward erosion

The lower drywell will be flooded in most cases as a result of either active injection systems such as the firewater addition system or via passive injection through the lower drywell flooder.

19EC.2.2.1 Core Concrete Attack (CCI)

This event characterizes the nature of core concrete attack. Three branches are considered.

- No CCI
- Wet CCI
- Dry CCI

The No CCI branch represents cases where there is little or no concrete attack. Wet CCI represents cases where CCI occurs in the presence of an overlying water pool. Dry CCI is for cases where the lower drywell was not flooded. The rate of CCI is higher for cases with dry CCI.

This event is a sorting type event which assigns a probability of 0 or 1 depending on the final branch taken in the CCI CET.

19EC.2.2.2 Suppression Pool Water Floods Lower Drywell after Downcomer Penetration (SP_INGRESS)

This event assesses if suppression pool water will flood into the lower drywell after the erosion front reaches the wetwell/drywell connecting vents. The vents are imbedded in the pedestal. If 25 cm of the pedestal concrete is eroded, the ablation front will reach the inner surface of the connecting vents. It is considered quite likely that this will result in water ingression and flooding of the lower drywell.

This event is only significant for Dry CCI sequences where the lower drywell is not flooded by either active injection or the passive flooder. The probabilities are assigned based on judgement.

19EC.2.2.3 Debris Flows From Lower Drywell to Suppression Pool after Downcomer Penetration (WW_DEB)

This event assesses whether a significant amount of the molten debris will flow from the lower drywell into the suppression pool following penetration of the wetwell/drywell connecting vents. After 25 cm of radial erosion the ablation front will reach the inner surface of the downcomers. The floor of the lower drywell is above the bottom of the connecting vents, which, in turn, are above the floor of the wetwell. Thus, once the downcomers are breached, a flowpath exists from the lower drywell into the suppression pool. Flow of a significant portion of the molten debris into the suppression pool will increase the debris surface area in contact with water and decrease the debris depth in the lower drywell. Although there is a great deal of uncertainty in this behavior, it is considered fairly likely that the debris will flow into the suppression pool.

19EC.2.2.4 Ratio of Radial to Axial Erosion (RAD_EROS)

Given that CCI is occurring, this event assesses the ratio of the radial concrete erosion to the downward erosion. Three branches are considered 1/5, 1/3 and 1/1. CCI experiments have generally demonstrated significantly more downward concrete penetration than radial penetration. It is hypothesized that radial erosion is limited because the concrete decomposition gasses establish a gas film between the debris pool and the concrete walls. This gas film acts to insulate the concrete sidewalls, and to convect debris heat upwards. This limits the heat transfer to, and ablation of, the concrete sidewalls. Conversely, the gas film at the bottom surface of the pool would be unstable due to the heavier overlying debris pool. The density difference would cause the lower gas film to collapse, allowing contact of the debris with the concrete. This difference in gas film behavior would limit the sideward heat transfer compared to the downward heat transfer.

In the BETA series of debris concrete experiments conducted at the KfK research center in Germany, downward erosion rates exceeded sideward erosion rates by a factor from 3 to greater than 5. For example, in the high power CCI experiment BETA V1.8, the downward erosion was measured to be approximately 40 cm and the sideward erosion was only about 2 cm

(1/20 sideward to downward erosion ratio). For the low power experiment V6.1, the downward erosion was 35 cm and the sideward erosion was 10 cm (1/3.5 ratio).

Based on the CCI experiments, and the generally accepted model described above, it seems appropriate to assume that downward erosion is strongly favored over sideward erosion. Consequently, larger probabilities are assigned to the 1/5 and 1/3 branches than for the 1/1 branch. However, since some residual uncertainty remains as to the appropriate assumption for the extent of radial erosion for large reactor scale situations, a small probability of is assigned to the 1/1 erosion branch.

19EC.2.2.5 Pedestal Failure (PED)

This branch assesses the probability of pedestal failure as a result of excessive radial concrete erosion of the lower drywell pedestal wall.

Structural analysis of the pedestal indicates that the loads can be supported without yielding if only the outer shell and 15 cm of the steel webbing remains intact. Thus, for a total wall thickness of 1.7 m, the lower limit for the amount of radial erosion which can be sustained without pedestal structural failure is 1.55 m. However, since the total depth of the pedestal is 1.7 m, erosion to the full 1.7 m depth will obviously result in pedestal failure. Additional discussion of the pedestal strength under radial concrete erosion is presented in Subsection 19EC.4.

Analyses were performed to estimate the extent of concrete erosion in the lower drywell under a variety of conditions. The results of these analyses are summarized in Subsection 19EC.5. Four cases were considered in the DET for quantification of pedestal wall failure. These cases are described below.

- Case 1—Debris Flows into Suppression Pool after Downcomer Penetration

  This case represents sequences where a substantial amount of the core debris relocates into the suppression pool after downcomer penetration. This is represented by deterministic calculations FMX100, FMXCSP and NFlood. The calculations indicate that the increase in the pool surface area results in either a coolable debris configuration, or greatly reduced radial erosion rates. Consequently, the likelihood of sufficient radial penetration to fail the pedestal in this case is considered to be remote.

- Case 2—Wet CCI With No Debris Flow into The Suppression Pool after Downcomer Penetration

  For sequences where CCI was predicted to occur in the presence of an overlying water pool with no debris relocation to the suppression pool, the maximum amount of downward concrete erosion at 50 hours was 1.55 m (Case FMX1P). Using this value for the amount of axial erosion, the radial erosion depth is estimated for the three cases. Comparing this

value to the pedestal capability of 1.55 m, estimates were made for the probability of pedestal failure.

- Case 3—Dry CCI With No Debris Flow into Suppression Pool and No Late Suppression Pool Water Ingression into The Lower Drywell

  This case represents case DRY in the deterministic analysis. In this case the debris is assumed to remain dry for the entire duration of the accident. No flow of either water or debris through the wetwell/drywell connecting vents is presumed to occur when the ablation front reaches the vents. For this case the axial ablation depth at 50 hours was calculated to be 2.5 m. Using this value to estimate the radial erosion depth for the three radial to axial erosion ratios, split fractions are assigned based on the pedestal capability.

- Case 4—Dry CCI With No Debris Flow into The Suppression Pool and Late Suppression Pool Water Ingression into The Lower Drywell

  The case in which the debris is initially dry, but becomes flooded with water after the ablation front reaches the wetwell/drywell connecting vents is considered to be slightly better than Case 3. In this case the debris is assumed to remain in the lower drywell throughout the period of CCI.

19EC.3 Deterministic Model for Core Concrete Interaction

As described above, several key parameters influence the potential for concrete erosion in the presence of an overlying water pool. An analytical tool was selected to investigate the impact that these parameters have on CCI, containment pressurization, opening of the overpressure protection system, and possible fission product release. MAAP-ABWR was selected since, with a few minor code modifications, it was capable of investigating the key parameters identified in the DET. MAAP-ABWR allowed the impact of parameter variations to be carried out through containment pressurization and fission product release.

A few simple code modifications were made to allow the user to control the debris coolability and to simplify the specification of the severe accident scenario. These changes are summarized below.

(1) Subroutine PLSTM was modified to allow the user to specify the upward heat flux. Model parameter, FCHF, was redefined to be the upward heat flux in Watts/m^2. All other debris-to-water heat transfer mechanisms were disabled in PLSTM.

(2) The following actions were added to the MAIN routine:

  (a) If lower drywell gas temperature exceeds 533 K - open passive flooder

  (b) If radial erosion exceeds 25 cm - allow debris to spread to wetwell and allow water to flood the lower drywell

(c) If radial erosion exceeds 50 cm (note that this limit is very conservative) - fail drywell with an area of ADWLEK (user input)

(d) If upper drywell wall surface temperature exceeds 533 K - begin to leak out of the upper drywell as specified in Subsection 19F.3.2.2

The major assumptions included in the MAAP analysis are described below:

(1) CCI experiments have generally demonstrated significantly more downward concrete penetration than radial penetration. It is hypothesized that radial erosion is limited because the concrete decomposition gasses establish a gas film between the debris pool and the concrete walls. This gas film acts to insulate the concrete sidewalls, and to convect debris heat upwards. This limits the heat transfer to, and ablation of the concrete sidewalls. Conversely, the gas film at the bottom surface of the pool would be unstable due to the heavier overlying debris pool. The density difference would cause the lower gas film to collapse, allowing contact of the debris with the concrete. This difference in gas film behavior would limit the sideward heat transfer compared to the downward heat transfer.

In the BETA series of debris concrete experiments conducted at the KfK research center in Germany, downward erosion rates exceeded sideward erosion rates by a factor from 3 to greater than 5. For example, in the high power CCI experiment BETA V1.8, the downward erosion was measured to be approximately 40 cm and the sideward erosion was only about 2 cm (1/20 sideward to downward erosion ratio). For the low power experiment V6.1, the downward erosion was 35 cm and the sideward erosion was 10 cm (1/3.5 ratio).

Based on the CCI experiments, and the generally accepted model described above, it seems appropriate to assume that the ratio of radial to axial attack is 1/5. However, this parameter is included as a parameter in the DET for pedestal erosion since the ratio is still uncertain.

Since MAAP assumed that radial and axial penetration were identical, the axial ablation numbers were multiplied by 1/5 to obtain an estimate on the radial attack depth.

(2) The heat transfer from the debris to the water was assumed to be equal to the user specified value throughout the transient.

Other than the changes described above, the standard MAAP-ABWR code was used to quantify the CCI decomposition event tree.

19EC.3.1 Minimum Heat Flux

The most critical element in determining the potential for core concrete interaction, and the containment response if it should occur is the minimum heat flux. The heat transfer between the water and the debris can be limited by:

(1) Conduction within the debris

(2) Critical heat flux

(3) Film boiling

The last is of concern if the debris surface temperature remains so hot that the water cannot wet the surface, i.e. if an insulating blanket of steam forms. Film boiling has been observed in well controlled laboratory environments using polished surfaces. However, it has also been observed that the smallest of surface imperfections or contaminants quickly results in a transition to nucleate boiling. It seems highly unlikely that the irregular surface of the debris would be able to maintain itself in film boiling. Therefore, film boiling is not likely to limit upward heat transfer.

Critical heat flux is sufficiently high that it would not impose a practical limit on debris coolability. Therefore, a lower limit on the upward heat flux may be obtained by consideration of the conduction limit. The biggest unknown is whether the debris remains in an intact slab-like configuration, an intact configuration with irregularities which increase the heat transfer area and act as fins, or if the debris develops cracks which allow water to ingress. The presence of cracks would increase the heat flux. Therefore, let us consider the worst situation (intact slab).

The temperature distribution in steady state, assuming one dimensional heat transfer and a homogeneous debris mixture, is given by:

$$k\frac{\partial^2 T}{\partial x^2} + q''' = 0 \qquad \text{(19EC-1)}$$

where:

k = thermal conductivity (3.5 W/mK for oxide debris)

q''' = volumetric heat generation

It is sufficient for our purposes to consider the case of 1% decay power. For a total debris mass of about 235,000 kg, this implies an average initial volumetric heat generation rate:

$$q''' = (1.5)\frac{MW}{m^3}$$

In a one-dimensional flat geometry, integrating Equation 19EC-1 twice yields:

$$T = \frac{-q'''x^2}{2k} + C_1x + C_2 \qquad (19EC\text{-}2)$$

If we

(1) Assume nucleate boiling is maintained at the surface

(2) Conservatively assume that the bottom of the debris in contact with concrete is adiabatic

(3) Impose the condition that the debris not ablate concrete and the temperature at the debris-concrete interface is 1550 K.

we obtain:

$$C_1 = 0$$

$$C_2 = 1550\ K$$

$$T(\delta_{lim}) = 450\ K$$

where:

δ_{lim} = debris thickness

Substituting into Equation , we have for the limiting debris thickness for coolability:

$$\delta_{lim} = 0.07\ m$$

This means that if we are in nucleate boiling at the surface, we can just remove decay heat purely by conduction through the debris slab at a thickness of 7 cm. The surface heat flux is:

$$q'' = q'''\delta_{lim} = 100 kW/m^2$$

The heat flux which would result from critical heat flux would be substantially higher than this value. Thus, one could view this as the lowest possible upward heat transfer given the boundary conditions. A higher temperature at the bottom of the crust or heat transfer into the slab would both increase the debris-to-water heat transfer.

This rather low heat transfer would be increased if the surface was of non-uniform thickness (fin effects) or especially if the surface cracked sufficiently to allow water to ingress.

19EC.4 Pedestal Strength

The configuration of the ABWR pedestal is shown in Figure 1.2-13e. The width of the pedestal is 1.7 m. The design consists of two concentric steel cylinders connected by steel web stiffeners. Ten wetwell-drywell connecting vents run through the annular region between the cylinders. The remainder of the space is filled with concrete. If significant core concrete attack occurs, the strength of the pedestal could be compromised as the pedestal is eroded. The strength of the pedestal after it has undergone erosion is examined to determine the maximum erosion depth allowable to ensure that the pedestal does not collapse.

The pedestal is designed based on the maximum stress obtained in the steel plates. The strength of the concrete is neglected. The allowable stress in the steel plates is 0.6 times the yield strength, neglecting temperature. The calculated stress without seismic loads in the ABWR pedestal is 0.4 times the yield strength.

For design analysis the largest single load is the accident temperature. If core concrete interaction were to take place as a result of a severe accident, the inner plate of the pedestal would melt. Without a continuous inner plate the moment induced by the differential temperature disappears. It is expected that any temperature induced moments acting along the stiffeners will be strain limited. Therefore, they will not reduce the capability of the outer plate.

In order to estimate the allowable ablation depth, the seismic and thermal loads are removed and the remaining loads are calculated. No attempt was made to take credit for the relocation of fuel from the vessel onto the floor of the drywell. The strength of the remaining concrete is neglected. The loads are compared to the yield strength of the remaining pedestal steel. Therefore, this calculation corresponds roughly to a service level C type of calculation.

The results of the calculation show that the outer shell of the pedestal plus 15 cm of the web stiffeners are required to maintain the pedestal loads below 90% of yield. This limit is used as a conservative estimate of the pedestal ultimate capability after erosion. The total pedestal width is 1.7 m. Therefore, pedestal integrity is ensured for ablation depths up to 1.55 m.

19EC.5 Application of CCI Model to ABWR

The deterministic code used for investigating core-concrete interaction in the ABWR was described in Subsection 19EC.3. This subsection will describe the evaluations that were made to support the quantification of the CCI decomposition event tree.

19EC.5.1 Sequence Selection

The MAAP-ABWR code, as modified for this application, allowed for a great amount of flexibility in analyzing the impact of key parameter variations on core-concrete attack. The following lists the key parameter variations that were investigated:

(1) Upward heat transfer to overlying water pool

(2) Mass of debris discharged from vessel

(3) Mode of fission product release from containment

(4) Flooding of lower drywell resulting from radial penetration of vertical connecting vents

(5) Debris spreading related to radial penetration of vertical connecting vents

The base case sequence selected to investigate core concrete interaction was the low pressure loss of injection scenario. This event was initiated by a transient with the assumption that all injection was unavailable. The RPV was depressurized manually when the core level dropped below 2/3 core height. Without coolant injection, the core melts and slumps into the lower vessel head. Local penetration failure occurs and the debris is discharged into the lower drywell. A radial to axial ablation rate of 1/5 is assumed in all sequences. Table 19EC-1 provides a chronology of the events up until the vessel is failed.

Table 19EC-2 defines each of the sequences analyzed and provides a summary of the results. The first column gives the case designation along with reference to specific notes. Columns two through four provide the relevant sequence definition information. For purposes of demonstration, all cases were executed for the dominant sequence, a low pressure loss of injection sequence with a containment pressure at the time of vessel breach of approximately 1 atm. The upward heat flux was varied between 100, 300, and 900 kW/m^2. A value of 100 kW/m^2 was selected to approximate the heat transfer associated with a stable crust formation where the upward loss is controlled by conduction of heat through the crust. A value of 300 kW/m^2 was selected to represent limited water ingression into the debris bed with the upward heat transfer being controlled by film boiling. The largest value used represents the critical heat flux limit for debris cooling. Further discussion of these values is included in Subsection 19EC.2.1.6

As run in its standard manner MAAP-ABWR calculates that 60% of the total core inventory was released from the vessel. The remaining 40% was calculated to be held up in the core with the decay heat being radiated to the vessel wall and convected into the upper drywell. The 40% remaining behind is typically the outer peripheral bundles which have low decay heat. To support the DET quantification, additional cases were run assuming that 100% of the core was discharged from the reactor vessel. This has two major influences on the containment behavior. Without the peripheral bundles in the core, the drywell heatup is reduced. Second, the added

core mass on the lower drywell floor will influence the calculation of core-concrete attack, debris coolability and containment pressurization.

19EC.5.2 Summary of Results

Table 19EC-2 summarizes the results of the deterministic analyses for the ABWR. The following general conclusions are indicated by these results:

(1) For all sequences with successful operation of the flooder, radial concrete erosion was less than the structural limit described in Subsection 19EC.4. Radial attack does not pose a significant challenge to containment.

(2) For sequences with operation of the containment overpressure protection system, due to suppression pool scrubbing, the fission product release is dominated by noble gas.

(3) Release times for cases with the passive flooder are on the order of 20 hours after the initiation of core damage (defined as onset of melting).

(4) The extended time period between vessel breach and rupture disk actuation (or containment failure) provides for a substantial reduction in the amount of fission product released from containment.

(5) Using experimentally-based values for the upward heat transfer (Subsection 19EC.1) would result in debris cooling in the ABWR and early termination of the core concrete attack. Therefore, the lower bound for upward heat transfer is conservatively assumed to be 100 kW/m^2. This is done in order to obtain substantial concrete erosion and demonstrate the robustness of the containment design if the debris is not quenched.

(6) For the dominant scenarios with successful operation of firewater to provide water to the debris, the time from onset of melting to fission product release is 24 hours from the beginning of the accident for all upward heat transfer rates.

A set of plots for case FMX100 case are included in Figures 19EC-3 through 19EC-7. This case demonstrates long-term core-concrete interaction, but is otherwise typical of the conditions analyzed. The depletion of zirconium in this case occurs at about 20,000 seconds, coincident with the onset of CO production. The hydrogen gas generation is not equivalent to the amount which would be generated from a 100% metal water reaction because of a competing reaction between the zirconium and CO_2.

19EC.5.3 Initial Concrete Attack due to Impinging Corium Jet

At vessel failure, core material is discharged from the RPV onto the floor of the lower drywell. At low RPV pressures, the discharge rate of the debris is controlled by gravity and the vessel breach area in the lower head. From analyses performed for FCI calculations, Subsection

19EB.6.2.2, it is assumed that ten penetrations failed. This results in a maximum corium discharge rate of 6000 kg/s. The total failure area is 0.145 m^2. Assuming a density for corium of 8000 kg/m^3, a discharge of 6000 kg/s corresponds to a corium velocity of 5 m/s. The following calculation estimates the initial concrete attack depth resulting from this impinging corium jet.

The model from the MAAP subroutine JET (Reference 19EC-9) was used to compute the concrete attack from an impinging jet of corium. The stagnation point heat transfer coefficient between the corium jet and the concrete is approximated by the expression,

$$Nu = \frac{hD}{k} = 1.14\sqrt{Re} \qquad (19EC\text{-}3)$$

or

$$h = 1.14 k_{cm} \sqrt{\frac{\rho_{cm} u_c}{\mu_{cm} D_{jet}}} \qquad (19EC\text{-}4)$$

where:

k_{cm} = Corium thermal conductivity

μ_{cm} = Corium viscosity

u_c = Velocity of the corium stream impinging on the floor

D_{jet} = Diameter of the jet

h = Heat transfer coefficient

ρ_{cm} = Corium density

Nu = Nusselt number

Re = Reynolds number

The corium velocity at the cavity floor is given by,

$$u_c = u_0 + g t_{fall} \qquad (19EC\text{-}5)$$

where:

u_0 = Velocity of the corium expelled from the reactor vessel

g = Acceleration of gravity

and t_{fall} is defined by

$$u_0 t_{fall} + \frac{1}{2} g t_{fall}^2 = z_v \quad \text{(19EC-6)}$$

where:

z_v = the elevation of the reactor vessel above the lower drywell floor.

A crust of frozen corium forms on the concrete and the ablation process is the same as at the reactor vessel penetration. Thus, the concrete ablation velocity is given by

$$u_{cn} = \frac{h(T_{cm} - T_{cnp})}{\rho_{cn}[c_{pcn}(T_{cnp} - T_0) + \gamma_{cn}]} \quad \text{(19EC-7)}$$

where:

T_{cm} = Bulk corium temperature

ρ_{cn} = Concrete density

c_{pcn} = Concrete specific heat

γ_{cn} = Concrete latent heat

T_{cnp} = Concrete melting temperature

T_0 = Initial concrete temperature

Substituting the corium velocity and the ABWR specific geometrical parameters into the above equations, results in an ablation rate of approximately 1 cm/s. With the debris being discharged over 5 seconds, the resulting ablation depth is 5 cm. This would only occur in the central portion of the lower drywell, and would in no way threaten the integrity of the structures.

19EC.6 Sensitivity to Various Parameters

Also included in Table 19EC-2 are other analyses that address possible sensitivities to modeling assumptions. These results are described below.

- Case DRY

  This case was run assuming that the passive flooder did not open and that, even after radial penetration of the vertical vent pipes, water was not introduced into the lower drywell. The

drywell began to leak as a result of high temperature at about 20 hours and resulted in a slow, low magnitude, release of fission products.

- Case DWFAIL

  This case is identical to case FMX300 except that the drywell was assumed to fail at the COPS set point. Due to the long time between vessel breach and containment failure, the fission products settle out very effectively and the result is a low magnitude release.

- Case FMX1P

  This case was identical to case FMX100 except that the debris is assumed to not spread into the wetwell after penetrating the vertical connecting vents. The results indicate little sensitivity to this assumption. The radial attack at 50 hours is 31 cm for a ratio of radial to axial attack of one to five.

- Case NFLOOD

  This case was identical to case ABWR100 except that the firewater addition system and passive flooder were not operational. Therefore, the debris was initially dry. After 25 cm of radial erosion, the debris was assumed to spread into the wetwell and water from the suppression was introduced into the lower drywell. The results indicate more concrete erosion with the COPS actuating at 17.4 hours compared to 19.1 hours.

- Case FIRE

  This sequence was identical to FMX100 except that the firewater system was used to add water to the debris. Due to the addition of cold water, the pressurization of containment due to steam was reduced and the COPS was not predicted to open until 24.6 hours as compared to 17.6 hours for the case with passive flooder operation.

- Case LATE

  This sequence was identical to case DRY except for a delayed vessel failure. The RPV was assumed to fail after all of the water in the lower plenum had boiled away and the debris heated up to the eutectic melting point (2501 K). Vessel failure occurred at 5.3 hours into the sequence as compared to 1.5 hours for the base case. Since there was no water discharged with the core debris at vessel failure, the gas temperature quickly increased to above the flooder actuation temperature. The flooder was assumed not to work for this case. The purpose of the run was to obtain an estimate of the time period between vessel failure and flooder actuation. The MAAP analysis conservatively assumes that the gas must reach 533 K before the flooder can open. In this case it took about one hour before the gas reached 533 K. Factoring in the difference between the wall surface and the gas temperature, the flooder would be expected to open within 30 minutes after discharge of the core debris. All other aspects of this run were similar to the DRY case.

The overall conclusions from the sensitivity analyses are that the ABWR containment design is quite insensitive to the uncertainties associated with core concrete interaction. The concrete erosion rates are consistent with other published results (Reference 19EC-8) and do not pose a serious threat to containment integrity. Operation of the COPS provides for a scrubbed release of the fission products and greatly limits the risk to the public.

19EC.6.1 Impact of Pedestal Concrete Selection

The pedestal of the ABWR is defined as the sidewalls of the lower drywell. This structure supports the vessel and the wetwell/upper drywell diaphragm floor. The type of concrete to be used in the pedestal is not specified. Concrete with low gas generation potential is required for the floor of the lower drywell.

Basaltic concrete was used for the lower drywell in determining the response of the containment to core concrete attack. This type of concrete is often used in the United States. The other type of concrete which is frequently used is limestone-common sand. Basaltic concrete is more rapidly eroded during core concrete interaction than is limestone-common sand concrete. Therefore, one would expect that if limestone-common sand concrete were used in the ABWR pedestal (i.e. the side walls), the sideward erosion would be slower than that presented in Table 19EC-2. Therefore, the estimates in that analysis for the times at which pedestal integrity could be threatened are expected to be conservative if non-basaltic concrete is used in the pedestal.

The other key impact of the type of concrete is the production of non-condensable gas. Limestone-common sand concrete produces more non-condensable gas than does basaltic concrete. However, this will not have a significant impact on this analysis because the surface area of the sidewall will be only 10-15% of the floor area if core concrete attack should occur. Furthermore, the shape of the debris pool will be pancake-like. The gas generated at the side wall will not be able to reach into the debris pool and cause more rapid metal water reaction in the debris pool. Rather, it will bypass the debris. Therefore, there will be little impact of the gas generation on the rate of attack due to any enhanced metal water reaction.

In summary, the type of concrete to be used in the pedestal side wall is not specified. If non-basaltic concrete is used in the pedestal the rate of sideward ablation may be somewhat reduced as compared to the analysis presented here. The rate of non-condensable gas generation may be slightly higher. However, because of the relative areas of the sidewall and the floor the impact will be small. The conclusions of the uncertainty analysis will not be affected by a different choice of concrete.

19EC.6.2 Impact of FMCRD Platform Grating

The FMCRD platform grating is located in the lower drywell at the elevation of the access tunnel. This rotating platform is circular and mounted on the rotating rail under the reactor vessel. There is an opening area at the center of the platform which is provided with traveling rail for the CRD handling device. Gratings will be installed on both sides of the rail for

maintenance personnel. Typically, the grating consists of 2.54 cm (1 inch) by 0.95 cm (3/8 inch) metal slats mounted edge-wise to form a grid with a grid size on the order of 2.54 cm (1 inch) by 5.08 cm (2 inch).

However, it is expected that the grating will quickly ablate due to the flow of debris. This is much the same as the ablation of the vessel bottom head as the debris leaves the vessel. Any late debris relocation would be a slow, drip-like movement which would fall straight through the ablated region of the platform. Therefore, debris will not be retained above the platform and there will be no impact on containment performance.

19EC.7 Impact on Offsite Dose

Cases with operation of the rupture disk are the only risk significant release categories which would be impacted by core concrete interaction (The other sequences are cases with early containment failure due to DCH.) The conclusion of the assessment is that CCI does not have significant impact on the offsite dose.

19EC.8 Conclusions

This attachment investigated the impact of core-concrete interaction on the ABWR containment response. First, detailed DETs were developed to address all of the key parameters that influence CCI. Then, several deterministic analyses were carried out to support quantification of the trees. The following summarizes the important conclusions of the CCI investigation:

(1) For the dominant core melt sequences that release core material into the containment, most result in no significant CCI. Virtually no sequences have dry CCI.

(2) Even for the low frequency cases with significant CCI, radial erosion remains below the structural limit.

(3) The fission product release mode for a sequence with CCI is dominated by operation of the containment overpressure protection system. The release, which occurs at about 24 hours, is not distinguishable from a case with no CCI.

(4) Experimental results indicate that sufficient upward heat transfer to an overlying water pool would exist in the ABWR lower drywell to cool the debris.

19EC.9 References

19EC-1 Final Report on Core Debris Coolability, IDCOR Task 15.2

19EC-2 "An Integrated Structure and Scaling Methodology for Severe Accident Technical Issue Resolution", to be published as NUREG/CR, Draft 1991.

19EC-3 G.A. Greene, C. Finfrock and S.B. Burson, "Phenomenological Studies on Molten Core-Concrete Interactions", Nuclear Engineering and Design, 108, 167-177, 1988.

19EC-4 M.W. Tarbell, D.R. Bradley, R.E. Blose, J.W. Ross, and D.W. Gilbert, "Sustained Concrete Attack by Low-Temperature Fragmented Core Debris", NUREG/CR-3024, SAND82-2476 R3, R4, July 1987.

19EC-5 R.E. Blose, J.E. Gronager, A.J. Suo-Antilla, and J.E. Brockman, "Sustained Heated Metallic/Melt Concrete Interactions with Overlaying Water Pools", NUREG/CR-4727, SAND85-1546 R3, R4, R7, July 1987.

19EC-6 R. Henry, "Experiments Relating to Drywell Shell - Core Debris Interaction", BWR Mark I Containment Workshop, Baltimore, MD, February 24-26, 1988. See also B. Malinovic, R. Henry, and B. Sehgal, "Experiments Relating to BWR Mark I Drywell Shell - Core Debris Interactions", ASME/AIChE National Heat Transfer Conference, Philadelphia, August 1989.

19EC-7 B.R. Sehgal, "ACE Program Phase D: Melt Attack and Coolability Experiments (MACE) Program", presentation at CSARP meeting, May 1992.

19EC-8 S.R. Greene, S.A. Hodge, C.R. Hyman, M.L. Tobias, "The Response of BWR Mark II Containment to Station Blackout Severe Accident Sequences", NUREG/CR-5565, ORNL/TM-11548, May 1991.

19EC-9 "MAAP 3.0 B Computer Code Manual", EPRI NP-7071-CCML, Volume 2, November 1990.

19EC-10 “ABWR Severe Accident Evaluations,” Toshiba UTLR-0014

Table 19EC-1 Summary of Timing for Core Concrete Interaction Base Case

Time (s)	Event
0.0	Loss of all injection
4.2	Reactor scrammed
1097.0	Core uncovered
1138.0	Manual depressurization
3451.0	Onset of core melt
5364.0	Slump into lower head
5382.0	Vessel failure

Table 19EC-2 Summary of CCI Deterministic Analysis for ABWR

Case #	Containment Press. at Vessel Failure (atmosphere)	Upward Heat Trans. (kw/m^2)	Debris Mass at Vess. Fail (Frac. of Tot. Inventory)	Radial Attack at 50 h (meters)	H2 Generated at 50 h (kg)	Time of FP Release (hours)	Mode of Release	Fission Product Release Fraction from Containment		
								NG	CsI	Sr
ABWR100	1	100	0.6	0.22	1813	19.1	COPS	1.0	2E-06	3E-09
ABWR300	1	300	0.6	9E-07	122	23.3	COPS	1.0	2E-10	2E-12
ABWR900	1	900	0.6	7E-06	122	23.2	COPS	1.0	3E-11	2E-12
FMX100	1	100	1.0	0.25	2130	17.6	COPS	1.0	1E-06	1E-08
FMX300	1	300	1.0	7E-03	154	19.3	COPS	1.0	1E-08	3E-15
FMX900	1	900	1.0	7E-04	111	19.1	COPS	1.0	1E-08	2E-14
FMXCSP*	1	100	1.0	0.25	2126	15.7	COPS	1.0	4E-07	3E-10
SENSITIVITY RUNS										
DRY	1	N/A	0.6	0.50	4990	19.8	DWT	0.34	4E-03	1E-05
DWFAIL	1	300	1.0	7E-03	154	19.3	DWF	1.0	8E-04	2E-10
FIRE	1	100	1.0	0.25	2131	24.6	COPS	1.0	5E-06	4E-10
FMX1P†	1	100	1.0	0.31	2762	17.6	COPS	1.0	1E-06	1E-08
NFlood‡	1	100	0.6	0.25	2127	17.4	COPS	1.0	8E-07	5E-10
LATE*f*	1	N/A	1.0	0.31	2697	20.0	DWT	0.23	6E-03	9E-09

* FMX100 Run with five times steel mass.

† Penetration into connecting vents does not cause debris spread.

‡ Flooder not operational; radial attack results in penetration to WW and debris spread.

f Vessel failure assumed to occur after lower plenum water boiled away and debris reheats.

COPS = Containment Overpressure Protection System

DWT = Drywell Leakage occurs through penetrations.

DWF = Drywell Failure (0.0973 m^2)

Figure 19EC-1 Core Debris Concrete Attack DET

Not Part of DCD (Refer to Reference 19EC-10)

Figure 19EC-2 Containment Event Evaluation DET for Pedestal Failure

Not Part of DCD (Refer to Reference 19EC-10)

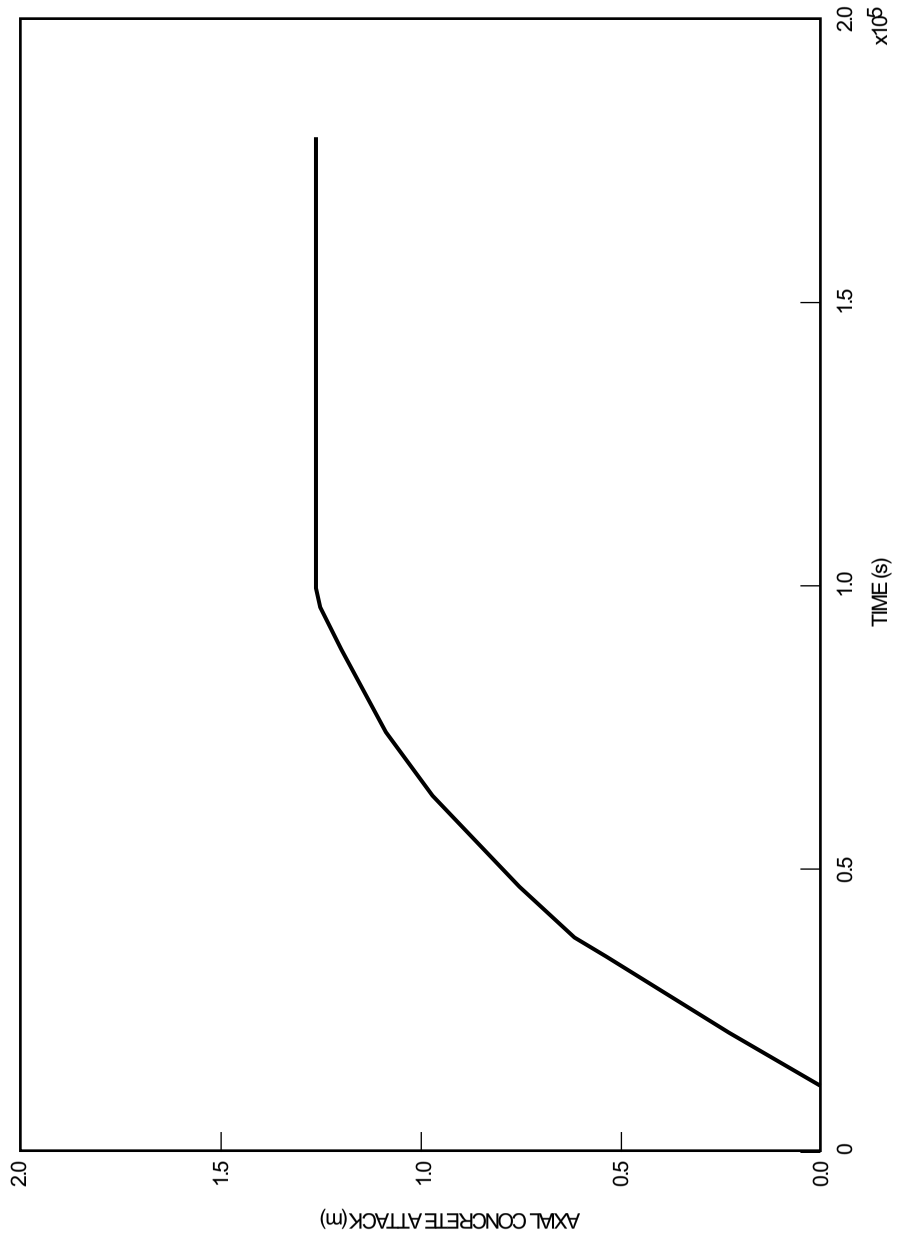

Figure 19EC-3 Sample Calculation for CCI Upward Heat Flux 100 kW/m^2: Axial Concrete Attack

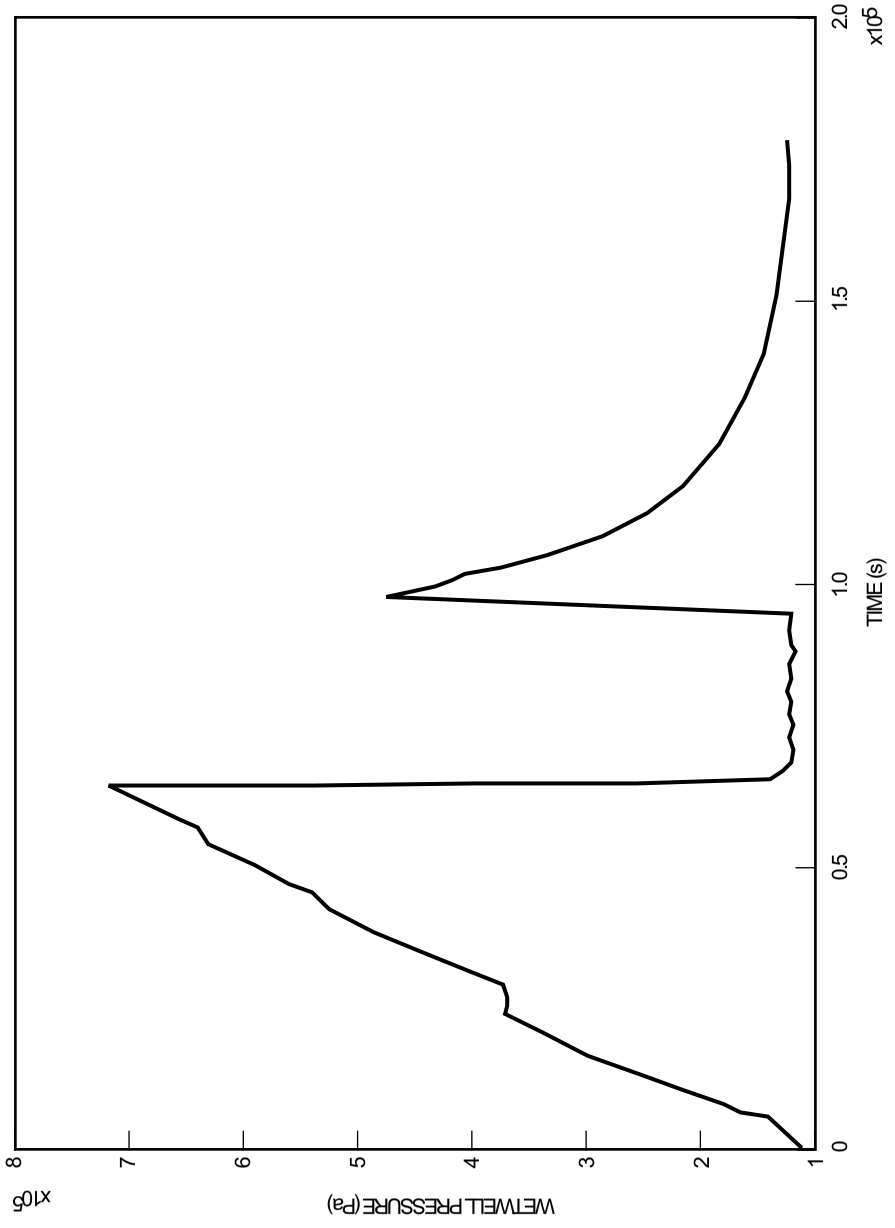

Figure 19EC-4 Sample Calculation for CCI Upward Heat Flux 100 kW/m^2: Wetwell Pressure

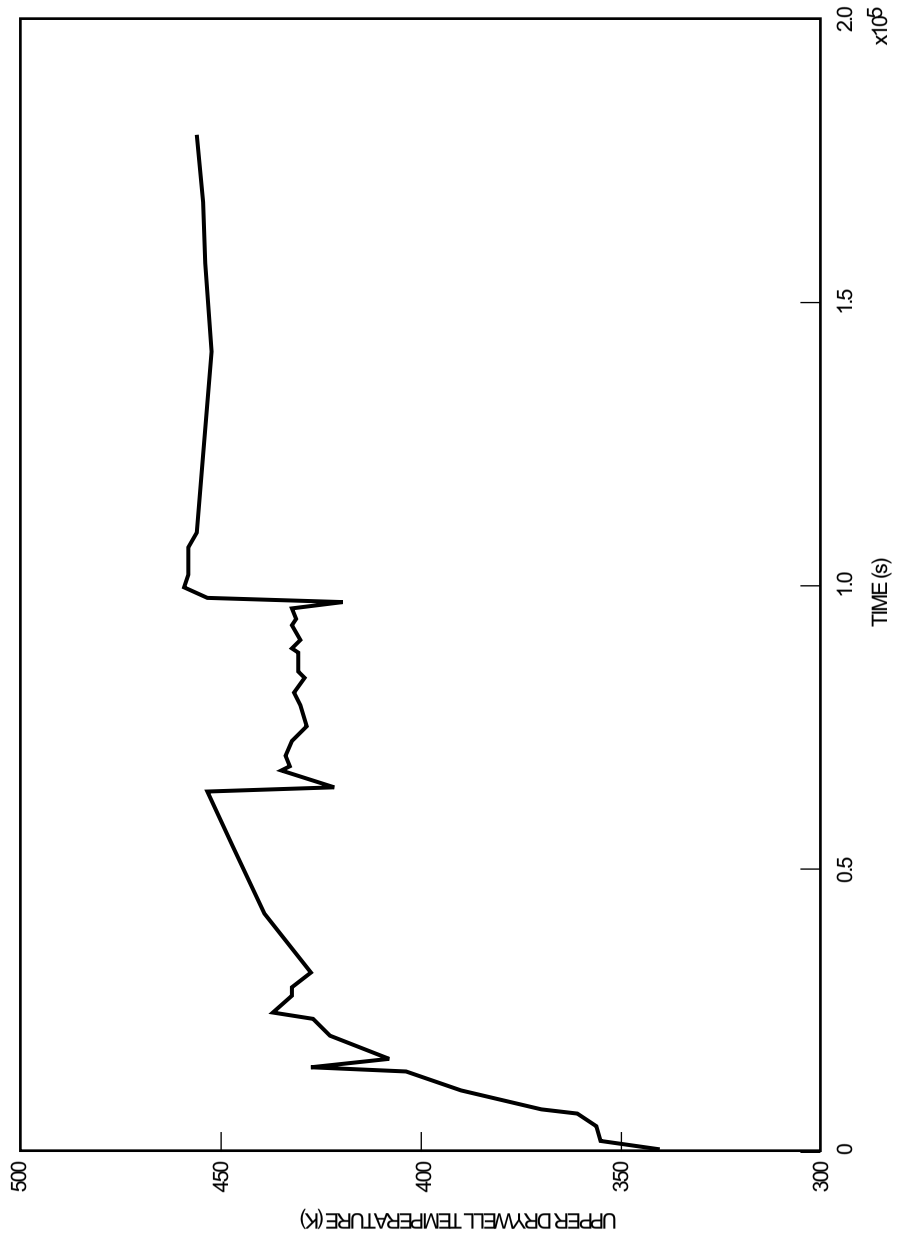

Figure 19EC-5 Sample Calculation for CCI Upward Heat Flux 100 kW/m^2: Upper Drywell Temperature

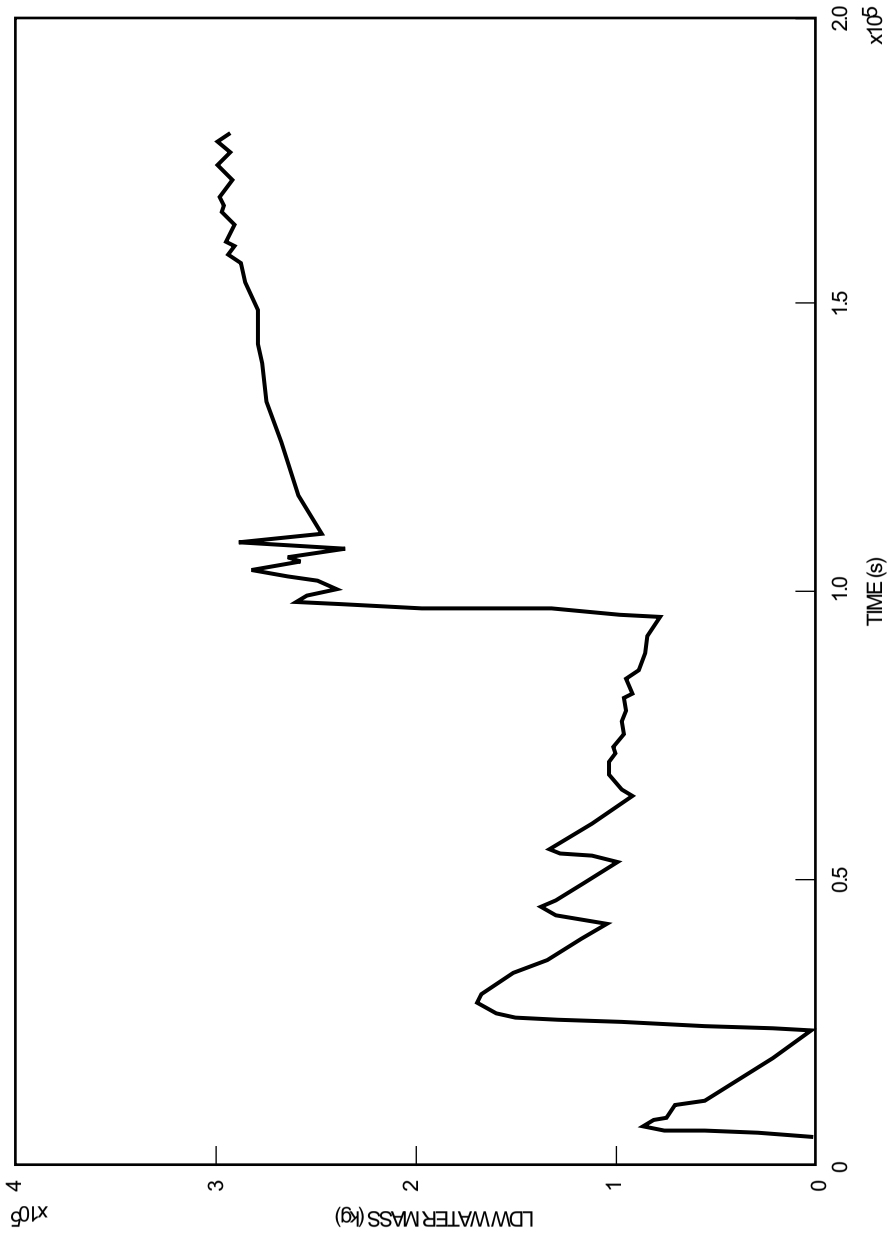

Figure 19EC-6 Sample Calculation for CCI Upward Heat Flux 100 kW/m^2: LDW Water Mass

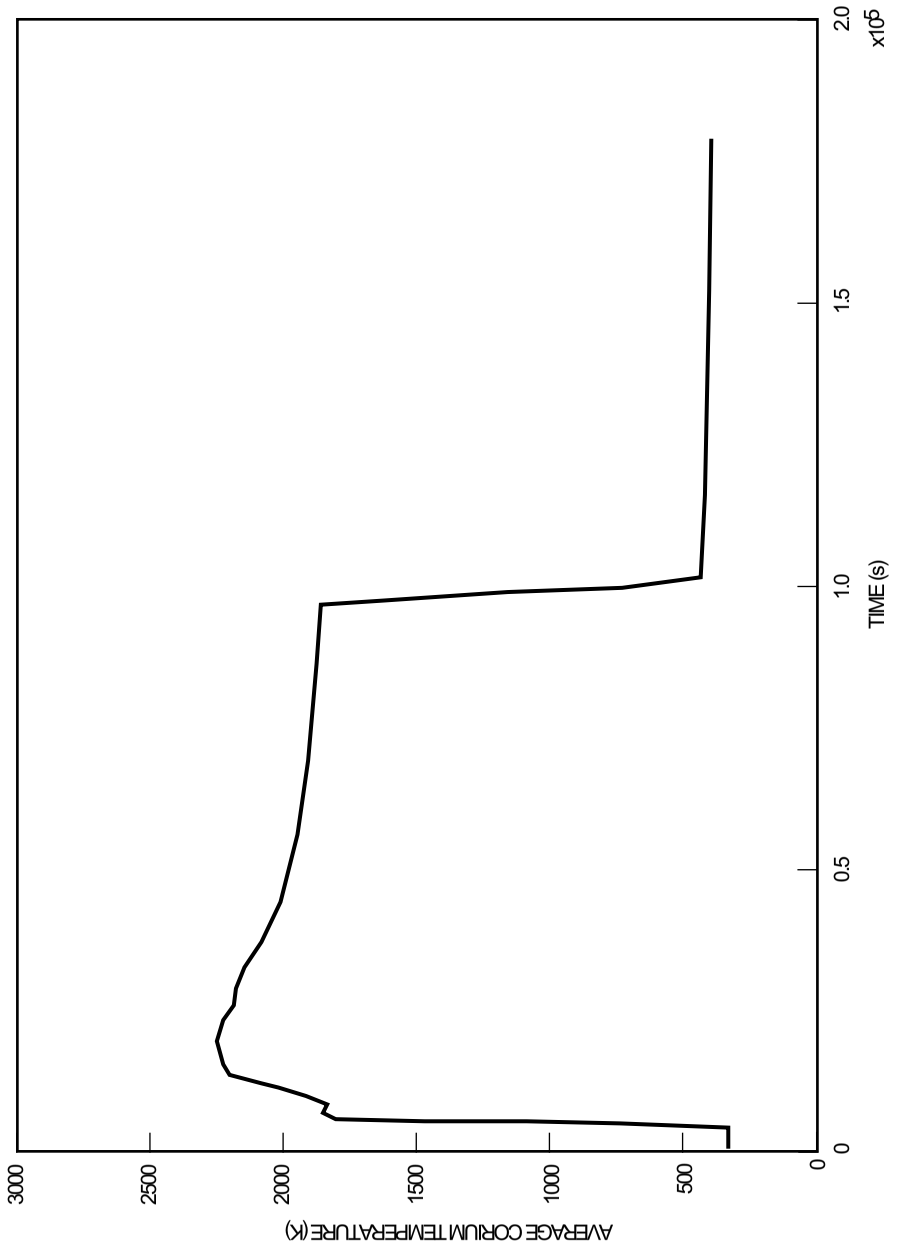

Figure 19EC-7 Sample Calculation for CCI Upward Heat Flux 100 kW/m^2: Average Corium Temperature

Figure 19EC-8 Not Used